NUKLEONIKA 2012;57(2):147–155

ORIGINAL PAPER

Polydiagnostics performed on high-tech plasmas

**Joost J. A. M. van der Mullen,
Jose M. Palomares,
Ekaterina Iordanova,
Simon Hübner,
Emile A. D. Carbone**

Abstract. The large effluxes generated by high-tech plasmas force plasmas to non-equilibrium conditions. This implies that plasma features are decoupled from each other and that therefore different methods have to be used quasi--simultaneously to characterize the plasma. Even more insight in plasmas and methods is obtained if polydiagnostics is applied to a series of plasma conditions that gradually differ in equilibrium departure. After discussing methods of passive and active spectroscopy, we apply polydiagnostics on an argon plasma operated in open air. By introducing H_2 and reducing the power we approach conditions of cool atmospheric plasmas (CAPs). It is seen that especially the passive methods for the electron temperature determination are very sensitive to the degree of equilibrium departure suggesting that active spectroscopy is preferable. However, one should realize that lasers can easily heat cool plasmas. This is due to the fact that the ionization degree of (semi-) CAPs is small.

Key words: polydiagnostics • high-tech plasmas • passive methods • active methods

J. J. A. M. van der Mullen✉, J. M. Palomares,
S. Hübner, E. A. D. Carbone
Department of Applied Physics,
Eindhoven University of Technology,
5600 MB Eindhoven, The Netherlands,
Tel.: +31 40 247 2550, Fax: +31 40 247 2555,
E-mail: j.j.a.m.v.d.mullen@tue.nl

E. Iordanova
Department of Applied Sciences,
Université Libre de Bruxelles (ULB),
50 F. Roosevelt Ave., CPI 165/04, Brussels, Belgium

Received: 26 November 2011
Accepted: 21 December 2011

Introduction

The increasing success of high-tech[a] plasma applications is based on the fact that plasmas produce large effluxes of photons and radicals. These are directed to application zones where they are used for the treatment of surfaces or volumes [12, 16]. However, generating large effluxes drives the plasma to non-equilibrium conditions; since transport will disturb the plasma balances of forward and corresponding backward processes [21]. The larger the effluxes are the larger the equilibrium--departure will be and the more the laws of classical statistical mechanics, ruled by the Boltzmann exponent $\exp(-E/k_BT)$, will lose validity.

A method often found to characterize non-equilibrium plasma conditions is to employ several new temperature-types. So, one can find expressions like $T_e > T_{ion} > T_{ex} > T_{vib} > T_{rot}$ showing that the electron temperature is larger than the temperature associated to ionization, excitation, vibration and rotation. One might wonder what the use of such a chain of inequalities is. Even if the temperature-values are given we remain with the question of the factual meaning of entities like T_{ex} or T_{ion}. A thermodynamic meaning in the sense of representing the mean energy of a certain particle-type is and can seldom be given. Nevertheless,

[a] with high-tech we refer to modern plasmas, i.e. plasmas used in the most advanced technology currently available.

this temperature inequality chain clearly shows that various plasma properties are decoupled; that is to say more or less independent of each other.

A more precise characterization of high-tech plasmas demands, apart from temperatures values, also the determination of the flux and number densities of active species. The best way to do that is by employing several different experimental techniques quasi-simultaneously. This polydiagnostic approach is needed since the departure from equilibrium makes different plasma aspects more independent, while the determination of independent plasma parameters in general asks for different techniques. Another reason is, that working on the edge of validity regimes, demands for a cross validation of different methods. Especially experimental methods based on equilibrium assumptions (like Boltzmann plots) will lose validity.

In this study we deal with passive and active spectroscopic methods and we will discuss how they perform as a function of equilibrium departure. Passive spectroscopy, also known as optical emission spectroscopy (OES), has the advantage that only the light produced by the plasma is analysed. So, in contrast to, for instance, electrical probe measurements the method is non-intrusive. The experiments are easy to perform but the interpretation of line and continuum radiation in terms of the main plasma properties is far from simple. Moreover, since OES methods are based on line-of-sight observations, we need inversion methods to get space resolved information.

The laser scatter techniques of Thomson (TS), Rayleigh (RyS) and Raman scattering (RnS), so-called active spectroscopic techniques, allow the simultaneous determination of the electron density n_e, electron temperature T_e and gas temperature T_{gas}. These methods, based on the scattering of laser photons by free and bound electrons, can be considered as direct techniques; meaning that the interpretation of signals created by TS, RnS and RyS does not depend (much) on the state of equilibrium-departure. Another advantage is that laser scattering techniques give plasma quantities with high spatial and temporal resolution. However, laser techniques are experimentally demanding and expensive. Moreover, care should be taken with the laser power; laser-plasma heating or even worse, laser-plasma creation, must be avoided.

We will compare the results of passive methods with each other and with those of the active group. The disagreement between the method-results can in many cases be attributed to the state of equilibrium departure. In this way polydiagnostics not only gives insight into the methods but also into the plasma. Special attention will be paid to discharges in open air and we will investigate how the experimental cross-validation will change as a function of power density and molecular loading. For low power densities, we will enter the regime of cool atmospheric plasmas (CAPs). These plasmas are popular nowadays because they are easy to operate. However, as we will show: they are not easy to characterize. The low power density and associated low electron densities will drive diagnostics to (and over) the edge of validity regimes. The low gas temperature (the plasma is "cool") will introduce molecule-like processes like van der Waals broadening and excimer formation. Moreover, the electron-atom (ea) interaction during laser scatter techniques will obscure the results of TS.

Experimental setup and techniques

The setup

Figure 1 gives a sketch of the setup used in our study showing diagnostics gathered around an atmospheric surface-wave induced plasma (SIP). This plasma, a semi-CAP, was studied in [14] were we changed the power density and introduced molecules in order to reach CAP conditions. This polydiagnostic setup is constructed in such a way that other techniques can be added while the plasma source can be replaced easily by

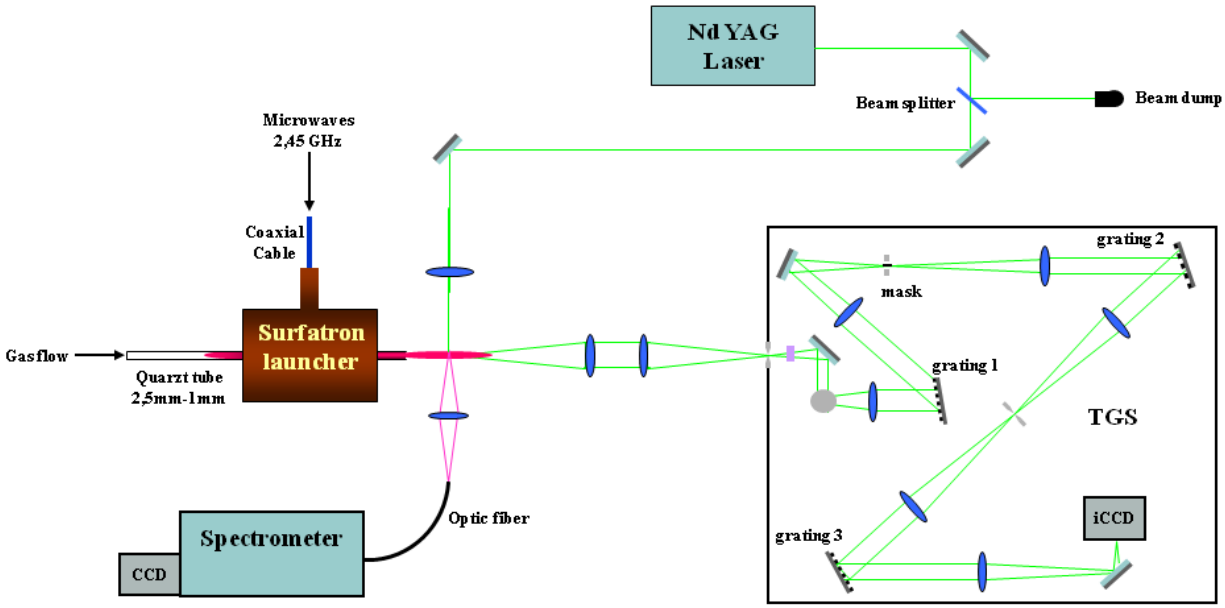

Fig. 1. Schematic view of the setup showing the plasma source (here an atmospheric surfatron), the laser, the active detection branch (TGS), and the passive detection branch (spectrometer). Note that the passive and active branches are not used simultaneously.

other plasma sources. For instance, in order to investigate how far plasma features depend on air entrainment or pressure we perform the measurements on another plasma source like a low-pressure SIP.

Passive spectroscopy

In this study, the OES methods consist of the measurement of line-broadening of the H_β line and absolute intensity measurements (AIM). The latter can be divided into absolute continuum and line intensity. In both cases the radiation is collected by a monochromator, while the intensities were calibrated using a tungsten ribbon lamp. For a more precise description of the methods, we refer to [5, 11].

Active spectroscopy

For the laser scattering techniques frequency doubled Nd:YAG lasers were used. The laser photons are (partially) scattered on either bound or free electrons, which creates respectively Rayleigh- and Thomson-scattered photons. The RyS along with a false stray light created by the scattering of the laser beam on nearby solid surfaces can be filtered out. For this purpose, we use a triple grating spectrograph (TGS) in which the combination of the two first gratings together with an intermediate mask forms a notch filter for the spectral range of 532 ± 0.2 nm. Only the spectrally broader signals of TS and RnS can pass this filter [18]. After the subsequent dispersion by the third grating, the photons are collected by an intensified-CCD camera (Andor iStar743). For more details, see, for instance, [14, 15, 22].

In TS the number of scattered photons is directly proportional to n_e; the calibration is obtained via RnS. On the other hand the Doppler broadening of the scattered photons gives an insight in the electron energy distribution, and therewith T_e. By removing the mask in the notch filter, we can use the same detection system to determine RyS. Ergo, the system can get quasi simultaneously n_e, T_e and T_{gas}. To unravel the RnS scattering on entrained air molecules from TS on electrons a fitting procedure needs to be employed. For this method, we refer to [22].

Experimental methods; features and pitfalls

Passive spectroscopy

Absolute line intensity (ALI) measurements

Figure 2 shows part of the argon atomic state distribution function (ASDF) of the semi-CAP described in Ref. [14]. It is constructed by combining the results of ALI measurements performed on several transitions together with the ground state density n_1 determined via the ideal gas law $p = n_1 k_B T_g$. In the same study we found n_e-values in the range of 10^{21} m^{-3}. For such reasonable high n_e-values, one can neglect the impact of radiation-escape on the ASDF. The electron-induced processes are frequent enough to compensate for

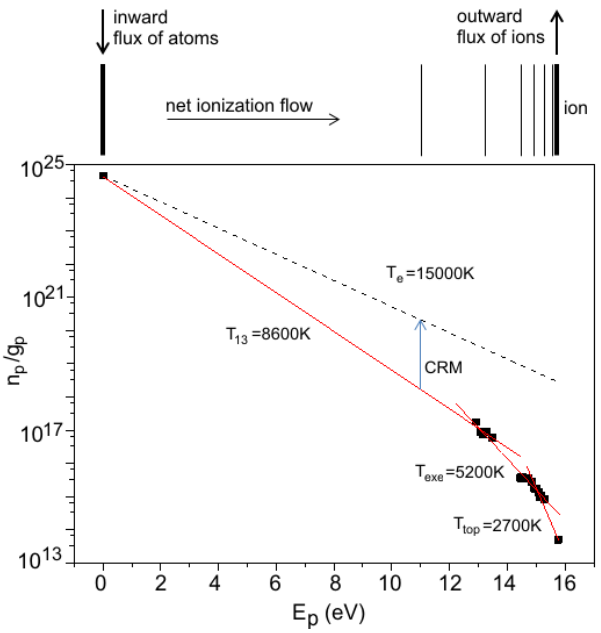

Fig. 2. A sketch of an ASDF typical of ionizing plasmas: 1) The efflux of ions has to be compensated by an inward flux of ground state atoms. 2) The sink of ions and source of ground state atoms leads to a net ionization flow through the atomic system which pushed the lower levels up and the higher down. By means of a CRM we can convert T_{13} into the electron temperature. This ASDF was found by experiments performed on the semi-CAP described in [14], but ASDFs of comparable shape have been found for many other plasmas.

the corresponding radiation-transport losses. This dominance of e-collision over radiative decay is often regarded as a justification to assume the presence of local thermodynamic equilibrium (LTE). However, the plasma being small in size will generate large effluxes of ei-pairs; and these will affect the ASDF inducing a variable shape. So, although e-collisions are dominant over radiative decay the plasma can be far from LTE in the sense that the ASDF strongly deviates from the equilibrium shape as prescribed by the Saha-Boltzmann equation.

The shape of the ASDF shown in Fig. 2, with its variable slope, is typical of ionizing plasmas. These are plasmas, or active plasma zones, in which the continuous loss of ei-pairs demands for (step-wise) ionization processes in order to guarantee a (quasi) steady plasma operation. Other examples of ionizing plasmas are those formed under low pressure conditions [5, 8]; the corresponding ASDF differs in absolute value, but has more or less the same shape. By means of an analytic collisional radiative model (CRM) based on hydrogen-like cross sections for e-induced transitions one can show that the ASDF slope at the location p in excitation space mainly depends on the ionization potential I_p of that location [19, 20].

$$k_B T_{slope} \approx I_p / 3 \quad (1)$$

Although the ladder-climbing stepwise ionization is driven by electron collisions we see that the temperature in the above equation has no thermodynamic meaning; it does not depend on the mean electron energy.

In Fig. 2 we indeed see that the slope changes drastically, the more we approach the continuum the steeper

the slope will be. This results from the fact that the flux in excitation space, preparing the creation of ei-pairs, is spread out over a diverging density of states[b] whereas the cross section for excitation increases[c] drastically.

In [1, 7] we presented a CRM dedicated to Ar with an analytical H-like top and a numerical bottom. In [5, 11] this CRM is employed to deduce the electron temperature T_e from the lower part of the ASDF. It basically is a two-step approach. In the first step the density per statistical weight $\eta(3) = n(3)/g(3)$ of the $4p$ levels, by short level "3", and the η-value of the ground state, level "1", delivered by the pressure $p = n_1 k_B T_{gas}$ are used to compute the temperature T_{13}. In the second step we employ a CRM to convert T_{13} into T_e.

We stress the fact that the density of the ground state cannot be obtained by OES; its absolute value is deduced from the pressure. Therefore, we have to determine the density of $\eta(3)$ in absolute way as well; the method of relative intensities does not lead to useful results.

In the conversion of T_{13} into T_e, where the CRM is employed, we need a value of n_e. This can be obtained from the absolute continuum intensity (ACI) measurements; see next section.

It should be mentioned that the use of CRMs for the determination of plasma parameters can be done in different ways, see, e.g. [10]. In [25] methods are given to get information on the structure of the electron energy distribution function EEDF.

Absolute continuum intensity (ACI) measurements

The above shows that temperatures derived from slopes of distribution functions or intensity ratios should be handled with care. This also holds for the classical method of T_e-determination using line/continuum ratios. This method can be used for plasmas in, or close to LTE. However, in ionizing plasma in which the density of the ions is pressed down, whereas the bottom part of the ASDF is pushed up (see Fig. 2) we can no longer expect reliable T_e-values. On the other hand we might expect the influence of the continuum generated in electron-atom (ea) interactions. This will be studied below.

The local source of continuum radiation is determined by the spectral emission coefficient $j_\lambda(\lambda)$ that can be obtained experimentally from the spectral intensity $I_\lambda(\lambda)$ and the size D of the plasma along the line of sight. The size D can be obtained by estimation or by means of an Abel inversion procedure. Theoretically, $j_\lambda(\lambda)$ is composed of three contributions:

$$(2) \qquad j_\lambda(\lambda) = j_\lambda^{ei,fb}(\lambda) + j_\lambda^{ei,ff}(\lambda) + j_\lambda^{ea,ff}(\lambda)$$

Here $j_\lambda^{ei,fb}(\lambda)$ represents the radiation generated during electron-ion (ei) recombination, $j_\lambda^{ei,fb}(\lambda)$ the free-free ei bremsstrahlung and $j_\lambda^{ei,ff}(\lambda)$ the free-free radiation created by ea-interactions. The two ei contributions can be taken together [9] as

$$(3) \qquad j_\lambda^{ei,fb}(\lambda) + j_\lambda^{ei,ff}(\lambda) = j_\lambda^{ei}(\lambda) = n_e^2 f_\lambda(\lambda,T_e)$$

where we assumed that $n_{ion} = n_e$ and introduced $f_\lambda(\lambda,T_e)$. Defining $g_\lambda(\lambda,T_e)$ such that

$$(4) \qquad j_\lambda^{ea,ff}(\lambda) = n_e\, n_a\, g_\lambda(\lambda,T_e)$$

we get, combining Eqs. (3) and (4) for the electron density the expression

$$(5) \qquad n_e = n_a\, g_\lambda (2 f_\lambda)^{-1} \cdot \{[1 + 4 j_\lambda^* f_\lambda/(n_a g_\lambda)^2]^{1/2} - 1\}$$

where $j_\lambda^*(\lambda) = I_\lambda(\lambda)/D$ is the measured value of the emission coefficient.

The cross sections for ei-interactions are, in general, much larger than those for ea-interactions. This implies that $f_\lambda >> g_\lambda$ and suggests that ea radiation can be neglected. However, for the plasmas under study the low ionization factor $\alpha = n_i/n_a$ will favour ea-over ei-continuum. A critical ionization degree for 532 nm is given by the expression

$$(6) \quad \alpha_{cont}^{crit} = g/f \approx 0.012\, T_e^3 - 0.027\, T_e^2 + 0.023\, T_e - 0.007$$

for the T_e range $0.6 < T_e < 3$ eV. For $\alpha < \alpha_{cont}^{crit}$, the ea interactions will rule the continuum. This is opposite to what is found in classical, that is LTE-like plasmas, such as arcs, shock tubes or astrophysical plasmas.

The values of $f_\lambda(\lambda,T_e)$ and $g_\lambda(\lambda,T_e)$ depending on T_e, have to be determined via ALI (section 'Absolute line intensity'). For the expressions of $f_\lambda(\lambda,T_e)$ and $g_\lambda(\lambda,T_e)$ and their T_e dependence, we refer to [9].

The AIM-method in which ALI and ACI are treated in an iterative way giving n_e and T_e was described and applied to a TIA plasma in [11]. In [8] it was used for plasmas created by a coaxial wave-guide. This AIM method can be applied to other plasma sources as well. If the plasmas are created in a different gas, e.g. He instead of Ar, one must change the functions $f_\lambda(\lambda,T_e)$ and $g_\lambda(\lambda,T_e)$, accordingly. If the plasma under study is populated by molecules one should take extra care. Indeed, the continuum part that is taken for the n_e-determination must be free from any atomic or molecular radiation.

Line broadening methods

The AIM method presented above gives values of the basic plasma parameters n_e and T_e with the advantage that the method is non-intrusive. One of the disadvantages is that absolute measurements have to be performed, meaning that the plasma radiation has to be calibrated with a standard light source. Most experimentalists find this cumbersome and prefer to work with relative instead of absolute intensities. However, this comes with the price that the plasma characterization loses validity.

If plasma parameters can be determined by line-shapes instead of intensities one can skip the calibration procedure. A well-known example is the Stark broadening of the H_β line. It provides a reliable method to determine n_e since the broadening, $\Delta\lambda_\beta$, is (almost) independent of other plasma parameters such as T_e. Other lines of the Balmer series, for instance H_γ, are

[b] The number of state per level, the statistical weight $g(p)$, scales with $I_p^{-1} I$.

[c] The cross section for electron atom collisions roughly scales with I_p^{-2}.

known to depend not only on n_e but also on T_e; in short $\Delta\lambda_\gamma = \Delta\lambda_\gamma(n_e,T_e)$. This means that a measured $\Delta\lambda_\gamma$-value represents a curve in (n_e,T_e) space. By measuring the broadening of two Balmer lines, for instance $\Delta\lambda_\gamma$ and $\Delta\lambda_\beta$, we get two curves in (n_e,T_e) space and the intersection determines a pair of n_e- and T_e-values.

This Stark intersection method (SIM) was successfully applied to argon plasmas created by the TIA [17]. However, the method fails for cooler plasmas. One of the reasons is that in CAPs the (atom) density is extra high. This favours van der Waals broadening that might compete with, or even dominate over Stark broadening. What remains valid for a large range of conditions is the H_β Stark broadening method so that, not T_e, but only n_e can be determined. However, CAPs subjected to power-reduction and/or molecule-entrainment will decrease so much in n_e that even the H_β-method tends to go below its validity regime, that is below the values for which theories are available. This theoretical lower limit is in the order of $n_e = 10^{20}$ m^{-3}. However, there where theories fail, one can use the polydiagnostic comparison to explore and extend the validity regime of the H_β method. Preliminary results in this field reported in [6] will be elaborated in [13] so that the H_β Stark broadening method can be extended down to $n_e = 10^{19}$ m^{-3}.

Active spectroscopy; laser scattering

The experimental procedures of Thomson, Rayleigh and Raman scattering were described in [6, 14, 15, 18]. Here, we focus on the T_e nature as determined by TS and the danger of laser-plasma heating.

The EEDF probed with TS

It was stated above that the characterization of non--equilibrium plasma conditions is often expressed by giving a manifold of T-definitions and -values. This rises the question in how far the T-definitions represent thermodynamically useful concepts. In that perspective we will discuss the nature of T_e(TS). Normally, the TS temperature is found using a procedure like the one given in [18] in which after baseline subtraction the TS spectrum is fitted with a Gaussian function. The half width of the distribution $\Delta\lambda_{1/e}$ gives T_e(TS) via $T_e = 5238\cdot\Delta\lambda^2_{1/e}$ (for perpendicular scattering of 532 nm laser radiation).

More insight in the T_e(TS)-nature is obtained if the logarithm of the signal P(δλ) is plotted as a function of $\delta\lambda = \lambda - \lambda_0$. As a Maxwellian EEDF leads to [24]:

$$P(\delta\lambda) = A \cdot \exp - \{m_e c^2 \delta\lambda^2/(4\lambda_o^2 k_B T_e)\} \quad (7)$$

where A is a proportionality constant, c the speed of light and λ_0 the laser wavelength, we expect that a plot of ln P(δλ) vs. $\delta\lambda^2$ gives a linear trend.

Figure 3b gives the result of the fitting procedure applied to the right wing of the curve given in Fig. 3a. It is evident that the scatter increases with δλ and that only the signal corresponding to relatively small δλ-values can be used to determine the temperature. From this example of the TS spectrum obtained from measurements performed on a low pressure SIP, we may conclude that the distribution can only be constructed from the first 3 nm of wavelength shift, which corresponds to kinetic energies of 4.5 eV [24]. However, a simple integration shows that this represents 95% of the electrons. We may thus state that T_e(TS) gives the bulk temperature of the electrons. One should therefore realize that the method depicted in Fig. 3b only represents the lower energy part of the EEDF and that TS does not give direct insight in the effect of argon ground state excitation. For this, we have to inspect the EEDF for energy values exceeding 12 eV. So, the creation of radicals and ei-pairs due to which we expect a depletion of the EEDF-tail, remains invisible for the TS procedure. In section 'Polydiagnostics for the T_e determination' we will show that comparing TS with the ALI method gives insight in the ei creation--power of the plasma and the effect on the EEDF.

Laser heating

Laser irradiation of plasmas will force electrons to oscillate. These systematic orbits are transferred into

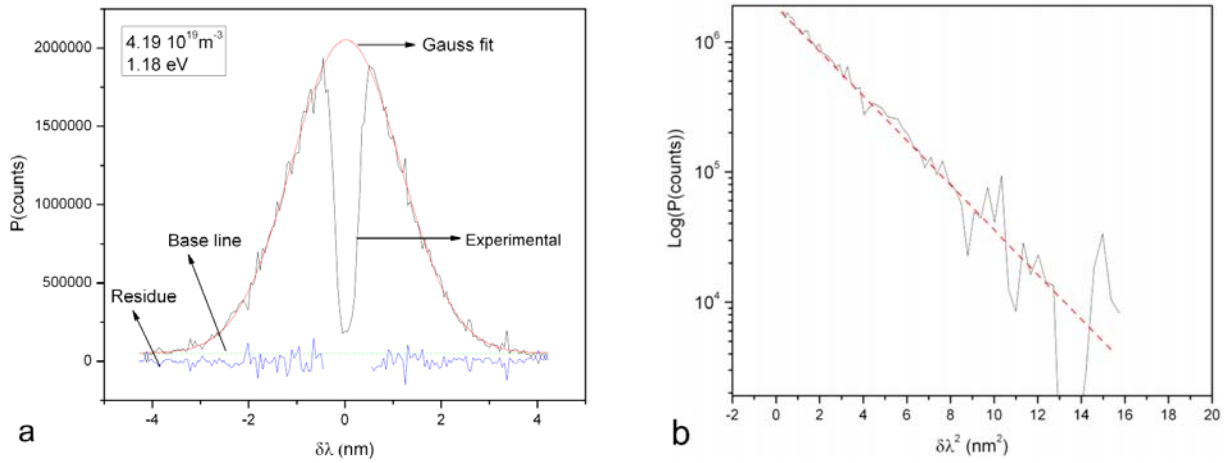

Fig. 3. The number of counts P(δλ) as a function of the wavelength shift $\delta\lambda = \lambda - \lambda_0$. Left: the measured P(δλ) (experimental) fitted by a Gaussian (Gauss fit) superimposed on a base line (base line). The gap in the central region around $\delta\lambda = 0$ stems from the blocking of the signal around the central wavelength; an action of the TGS that is needed to reduce the influence of Rayleigh photons and false stray light, i.e. at $\lambda = \lambda_0$. Right: The logarithm of P(δλ) plotted vs. $\delta\lambda^2$ after baseline subtraction showing the expected linear tendency for the first 7 nm^2. For higher δλ-values, the noise obscures the signal.

stochastic motions, thus heat, if electrons collide during these oscillations. The amount of heat generated in that way depends on the laser energy $\mathcal{E}$, the cross section $\mathcal{A}$ of the laser beam and the rate of the electron collisions with heavy particles. The formulas for laser heating given in the literature are almost exclusively based on ei-collisions. However, in CAPs where the neutral density is high, we find that ea-interactions are much more important. Compared to the classical ei-induced heating we get an enhancement of $(n_a k_{ea})/(n_e k_{ei})$, where $k_{ea}(k_{ei})$ stands for the rate coefficient for momentum transfer from electrons to atoms (ions). For CAPs, this factor $(n_a k_{ea})/(n_e k_{ei})$ can easily amount to 10^2. From this, we can obtain a critical ionization degree below which the ea induced heating is more important than the ei contribution [2]

$$(8)\quad \alpha_{heat}^{crit} = k_{ea}/k_{ei} \approx 3.4 \cdot 10^{-5}(T_e^{3/2})(1 + 6.4T_e + 14.2T_e^2)$$

where T_e is expressed in eV. This form of Ohmic heating is also known as inverse bremsstrahlung (IB) and the fact that for CAPs the heating due to ea-interactions dominates over that created by ei-interactions and is closely related to the dominance of the ea continuum treated in section 'Absolute line intensity (ALI) measurements'.

The increase of the T_e due to the laser action can be controlled by tuning the laser power. Calculations and experiments show that for the semi-CAPs under study the laser fluency $\mathcal{F} = \mathcal{E}/\mathcal{A}$ should not exceed 10^6 J/m^2, a value that corresponds to a pulse energy of only 10 mJ focused on a focal area of 10^{-2} mm^2. This fluency is small in comparison to what is usually used in LIF, TALIF and TS experiments. So, care must be taken in the interpretation of the corresponding results.

Polydiagnostic comparison

The methods treated in previous sections can be used to investigate several types of plasmas. Most insight in the methods and plasmas is obtained if measurements are performed (quasi) simultaneously. In [3] we performed polydiagnostics on an inductively coupled plasma; in [4, 13] such a study is reported for a low pressure SIP. In this section we initially follow [14] in a polydiagnostic study performed on a semi-CAP in which CAP conditions are approached step-by-step. To that end the semi-CAP was subjected to three plasmas conditions A, B, C. In case A the plasma is generated by coupling 74 W to a pure argon flow. In case B and C we applied 88 W and 57 W, respectively to an argon flow at which 0.3% of H_2 was admixed. For all three settings, the plasma was observed at a 1 mm distance from the origin of the torch. The sequence A → B → C is that of approaching CAP conditions; i.e. the gas temperature decreases.

Polydiagnostics for the n_e determination

Figure 4a shows the n_e results for the three different methods: Thomson scattering (TS), absolute continuum intensity (ACI) measurements and H_β Stark broadening. The agreement is good; all methods show the same decrease in n_e while approaching CAP conditions. By approaching CAP conditions even further and performing polydiagnostics at each stage it is possible to extend the H_β method to n_e-values below those for which theoretical methods are available. This is the aim of [13].

Polydiagnostics for the T_e determination

Figure 4b, giving the results of the T_e-values obtained with TS and ALI, shows a reasonable agreement for A and B, but a disagreement for case C. Approaching CAP conditions apparently induces an increase in T_e(TS), whereas T_e(ALI) remains more or less constant. A subsequent study [23] on the same semi-CAP shows that the T_e(TS) also increases for increasing z-values; i.e. distances to the launcher. Since one of the reasons for the discrepancy T_e(TS) > T_e(ALI) might lay in a possible destruction of excited Ar levels by (entrained) molecules we studied pure Ar plasmas; thus isolated from the environment. To that end argon SIPs were used operating at lower pressures in the range of 6–20 mbar. The TS and ALI measurements were done as a function of axial positions. In comparing the results of three studies: 1) the semi-CAP at the fixed z-value following A → B → C, 2) the semi-CAP for different z-values and 3) intermediate pressure SIPs for different axial positions we found the same trend: the T_e(TS) increases if the ionization ratio $\alpha = n_e/n_a$ decreases; whereas T_e(ALI) remains more or less constant.

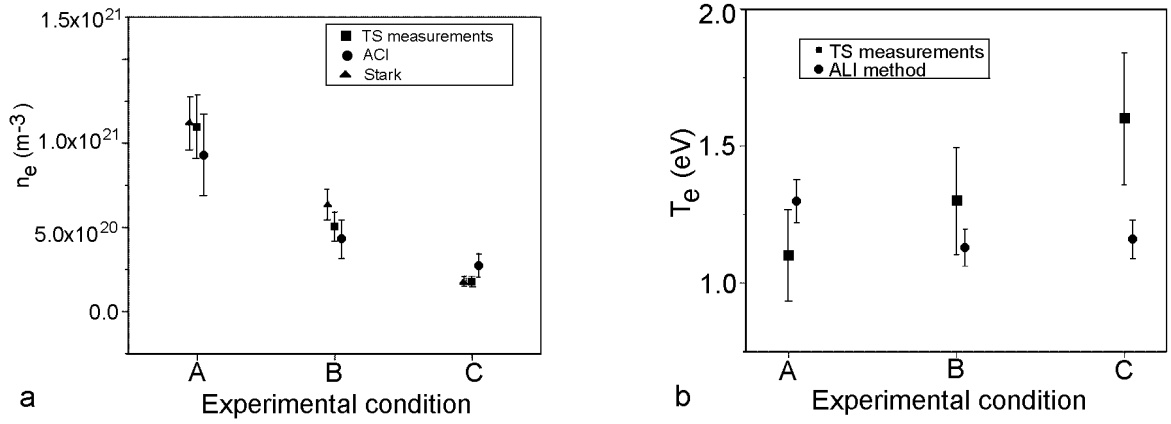

Fig. 4. For the three conditions A, B, and C we show left n_e obtained by the three different methods given in the legenda; and right T_e delivered by two methods.

The understanding of this trend in which α again plays a key role can best be studied by applying the electron particle balance (ePB) to the findings in experiment 3). This ePB reading

$$(9) \qquad n_e n_1 k^*_{ion}(T_e) = -\nabla(D_{amb}\nabla n_e) = D_{amb}\, n_e R^{*-2}$$

states that the diffusive efflux of ei-pairs has to be delivered by effective ionization. Here $k^*_{ion}(T_e)$ stands for the effective ionization rate coefficient, while D_{amb} is the ambipolar diffusion coefficient. In the last equation-member we replaced the double action of the ∇ operator by a division by R^{*2}, that is the square of the effective discharge radius. The ePB sets a strict demand for T_e due to the strong dependence of $k^*_{ion}(T_e)$ on T_e and it is clear that steeper gradients (small R^*-values) and higher diffusion coefficients demand for higher T_e-values; these are needed for the higher ei-pair creation demands to sustain larger effluxes.

In conditions of relatively high α-values we found good agreements between the T_e-values measured by ALI and TS [4] and the T_e demanded by ePB based on a Maxwellian k^*_{ion}, hereafter shortly by the Maxwellian-ePB. However, for low α-values a discrepancy is found between the Maxwellian ePB and ALI on the one hand and TS on the other hand.

This dependence on α points towards the study reported [20] where it was found that α plays an important role in the criterion for the presence of Maxwell equilibrium. This equilibrium is present provided that

$$(10)\ \alpha >> \alpha^{crit}_{max} \text{ with } \alpha^{crit}_{max} = C(S)\,(2\ln\lambda_c)^{-1}\,(k_B T_e/E^*_{12})^2$$

In the case of argon we have C(Ar) = 0.3 and E^*_{12} = 12 eV. Inserting for the Coulomb logarithm $\ln\lambda_c = 7$ and $k_B T_e = 1.2$ eV we find that $\alpha^{crit}_{max} = 2 \times 10^{-4}$. Inspecting Fig. 4 where we find for condition C typically $n_e = 2.5 \times 10^{20}$ m^{-3}, whereas $T_g = 1400$ K and $p = n_1 k_B T_{gas} = 1$ bar gives a gas density $n_1 = 5 \times 10^{24}$ m^{-3} so that $\alpha \approx 5 \times 10^{-5}$. Thus the criterion given in Eq. (10) is not fulfilled, meaning that departures from a Maxwell EEDF can be expected. The Coulomb collisions between electrons are not able to compete with the loss of high energy electrons as demanded by a Maxwellian rate. This leads to an EEDF with a broken tail.

The statements given above that ePB puts a demand on T_e, need some refinement: for a Maxwellian EEDF the ePB dictates the T_e value, such that large ei effluxes demand for high T_e values; however, for a non-Maxwellian EEDF with a broken tail an even higher T_e (better: mean energy) is demanded since a tail-depleted EEDF needs a higher mean energy to generate the same ei-pairs creation. Since T_e(TS) probes the bulk (the mean energy) it will go up.

The fact T_e(ALI) does not change (much) for decreasing α-values suggests that T_e(ALI) probes the efflux; i.e. it is directly connected to the last member of Eq. (9) which does not change if we increase the axial position. The radius and diffusion coefficient remain unaltered. So, T_e(ALI) probes the creation of ei-pairs and can best be denoted by the creation temperature.

The relation with the line intensity of the 4*p* level can be understood better by realizing that the ionization is mainly stepwise with the level block 4*p* as important intermediate station. Therefore, the 4*p* radiation, and thus T_{13}, probes the ionization flux in excitation space and thus the ei-pair creation. So, concluding T_e(TS) = T_{bulk} and T_e(ALI) = $T_{creation}$; at high α-values, under Maxwell equilibrium, these temperatures are the same. Low α-values force T_{bulk} upward, whereas $T_{creation}$ remains (almost) the same.

Approaching CAP conditions more closely

In Ref. [14] we could reach semi-CAP conditions with central gas temperatures of around 1400 K. This is relatively low, but still too high for soft surface treatment such as wound healing. On the contrary, by personal experience we found that the semi-CAP is more suitable for wound creation than for wound healing; real CAP conditions were not reached. Nevertheless, the trends observed in the study of gradual approach can be extended to predict what happens at further cooling. This will be discussed using the following schematic energy flow

$$\begin{array}{rll} & \rightarrow \{h^*\} \rightarrow \text{radicals} & \text{inelastic} \\ \{EM\} \rightarrow \{e\} \rightarrow & \{h\} \rightarrow \text{heat} & \text{elastic} \end{array}$$

showing that electrons heated by the electromagnetic field will use part of their energy in the elastic branch for the heating of heavy particles {h} and part for the creation of radicals {h*} in the inelastic branch. If the power density is reduced or if the {h*} branch is enhanced due to the introduction of molecules, we can expect that the electron density goes down. This is associated with a reduction of T_g and thus with an increase of the gas density n_a. This will favour the ea-over the ei-continuum and facilitate laser-plasma heating. Another consequence of the corresponding decrease in α is a further depletion of the EEDF tail. This means that the T_e(TS) (the bulk temperature) must go up. The performance and interpretation of TS will be obscured since a low n_e implies that we approach (or exceed) the TS detection limit since the weak (low n_e) and broad (high T_e) signal will be embedded in a large ea continuum. Applying high laser powers is not an option since that will induce laser heating.

So, active spectroscopy on CAPs will be difficult and the solution is to extend polydiagnostics in gradual approach as far as possible. In such a study we need to calibrate OES step-by-step and employ for TS a high rep-rate laser producing low energy pulses of short duration. The former is needed to avoid laser heating the latter since the smaller the measurement-time the less we are hindered by plasma light.

Summary and conclusions

The application of emission spectroscopy deducing temperatures from relative intensities, using a Boltzmann plot, does not give insight. More information is obtained if absolute intensities of the line and continuum emission are combined. A better solution is to use laser aided diagnostics, but then we have to avoid laser heating of the plasma. The best is to combine various methods

and to perform polydiagnostics for a series of plasma conditions for which equilibrium departure is changed gradually.

We started the study by a discussion of the pros and cons of three passive methods, Stark broadening and the absolute intensity measurements (AIM) of the continuum (ACI) and line emission (ALI). After that, we discussed Thomson scattering (TS). Special attention was paid to the nature of the electron temperature as determined by TS and the danger of plasma laser heating. A mechanism that is often overlooked for plasmas with low degree of ionization.

Equipped with the background knowledge of the various methods we performed a gradual polydiagnostic approach study with a semi-CAP moving toward CAP conditions by reducing the power and adding H_2 molecules. Comparing the results approaching CAP conditions gave an insight in the validity of the various methods and in the plasmas in question.

For the case of the electron temperature, the agreement found in the results of TS and ALI on an almost pure argon plasma suggests that ALI provides a reliable method for the T_e determination for moderate non-equilibrium conditions. However, when H_2 is introduced and the power is reduced, we see that the agreement between ALI and TS becomes worse. The temperature values obtained by TS are systematically larger than those given by ALI. A comparison with the results obtained on a low pressure surfatron suggests that the most likely reason for this discrepancy is that the tail of the electron energy distribution function (EEDF) gets depleted when the ionization fraction decreases. Theoretical considerations make clear that the ionization ratio $\alpha = n_e/n_a$ is the key parameter and that low α-values create an EEDF with a broken tail. Such a tail-depleted EEDF demands for a higher mean energy for the same creation of ei-pairs. As T_e(TS) measures the mean energy, whereas T_e(ALI) probes the ei-creation of the plasma we can understand why T_e(TS)/T_e(ALI) will increase approaching CAP conditions, since in that approach α will go down.

Acknowledgment. This work, supported and financed by the Dutch Technology Foundation STW and ECN, is performed in the framework of the bilateral relation between the Universities in Eindhoven (the Netherlands) and Cordoba (Spain) and embedded in the Belgian Federal Government Interuniversity Attraction Pole project PAI-VI/08 'Plasma Surface Interactions'.

References

1. Benoy DA, van der Mullen JJAM, van der Sijde B, Schram DC (1991) A novel collisional radiative model with a numerical bottom and an analytical top. J Quant Spectrosc Radiat Transfer 46:195–210
2. Carbone EAD, Palomares JM, Hübner S, Iordanova E, van der Mullen JJAM (2012) Revision of the criterion to avoid electron heating during laser aided plasma diagnostics (LAPD). J Instrum 7;1:C01016
3. De Regt JM, de Groote FPJ, van der Mullen JJAM, Schram DC (1995) Comparison of active and passive spectroscopic methods to investigate atmospheric inductively coupled plasmas. Spectrochim Acta B 51:1371–1383
4. De Vries N (2008) Spectroscopic study of microwave induced plasmas. PhD Thesis, Eindhoven University of Technology, The Netherlands
5. De Vries N, Iordanova E, Hartgers A *et al.* (2006) A spectroscopic method to determine the electron temperature of an argon surface wave sustained plasmas using a collision radiative model. J Phys D: Appl Phys 39:4194–4203
6. De Vries N, Palomares JM, Iordanova E, van Veldhuizen EM, van der Mullen JJAM (2008) Polydiagnostic calibration performed on a low pressure surface wave sustained argon plasma. J Phys D: Appl Phys 41:205203
7. Hartgers A (2003) Modeling of a fluorescent lamp plasma. PhD Thesis, Eindhoven University of Technology, The Netherlands
8. Hübner S, Wolthuis J, Palomares JM, van der Mullen JJAM (2011) Investigating a coaxial linear microwave discharge. J Phys D: Appl Phys 44:385202
9. Iordanova E, de Vries N, Guillemier M, van der Mullen JJAM (2008) Absolute measurements of the continuum radiation to determine the electron density in a microwave-induced argon plasma. J Phys D: Appl Phys 41:015208
10. Iordanova S, Koleva I (2007) Optical emission spectroscopy diagnostics of inductively-driven plasmas in argon gas at low pressures. Spectrochim Acta Part B 62:344–356
11. Iordanova E, Palomares JM, Gamero A, Sola A, van der Mullen JJAM (2009) A novel method to determine the electron temperature and density from the absolute intensity of line and continuum emission: application to atmospheric microwave induced Ar plasmas. J Phys D: Appl Phys 42:155208
12. Moisan M, Barbeau J, Crevier M-C, Pelletier J, Philip N, Saoudi B (2002) Plasma sterilization. Methods and mechanisms. Pure Appl Chem 74;3:349–358
13. Palomares JM, Hübner S, Carbone EAD *et al.* (2012) Stark broadening calibration with Thomson scattering at low density cold plasmas. (submitted to Spectrochim Acta B)
14. Palomares JM, Iordanova E, van Veldhuizen EM *et al.* (2010) Atmospheric microwave-induced plasmas in Ar/H_2 mixtures studied with a combination of passive and active spectroscopic methods. J Phys D: Appl Phys 43:395202
15. Palomares JM, Iordanova E, van Veldhuizen EM *et al.* (2010) Thomson scattering on argon surfatron plasmas at intermediate pressures: Axial profiles of the electron temperature and electron density. Spectrochim Acta B 65:225–233
16. Rath JK (2003) Low temperature polycrystalline silicon: a review on deposition, physical properties and solar cell applications. Sol Energ Mat Sol C 76:431–487
17. Torres J, Palomares JM, Sola A, van der Mullen JJAM, Gamero A (2007) A Stark broadening method to determine simultaneously the electron temperature and density in high-pressure microwave plasmas. J Phys D: Appl Phys 40:5929–5936
18. Van de Sande MJ (2002) Laser scattering on low temperature plasmas-high resolution and stray light rejection. PhD Thesis, Eindhoven University of Technology, The Netherlands
19. Van der Mullen JJAM (1990) Excitation equilibria in plasmas; a classification. Phys Reports 191:109–220
20. Van der Mullen JJAM, Broks BHP (2005) Disturbed bilateral relations: a guide for plasma characterization and global models. J Phys: Conf Series 44:40–52
21. Van der Mullen JAAM, Jonkers J (1999) Fundamental aspects of comparison of non-equilibrium aspects of ICP and MIP discharges. Spectrochim Acta B 54:1017–1044
22. Van Gessel AFH, Carbone EAD, Bruggeman PJ, van der Mullen JJAM (2011) Simultaneous Thomson and Raman scattering on an atmospheric-pressure plasma jet. IEEE Trans Plasma Sci 39:2382–2383

23. Van Gessel AFH, Carbone EAD, Bruggeman PJ, van der Mullen JJAM (2012) Laser scattering on an atmospheric pressure plasma jet: disentangling Rayleigh, Raman and Thomson scattering. Plasma Sources Sci Technol 21:015003 (9 pp)
24. Warner K, Hieftje GM (2002) Thomson scattering from analytical plasmas. Spectrochim Acta B 57:201–241
25. Zhu X, Pu Y (2011) Determination of non-Maxwellian electron energy distributions in low-pressure plasmas by using the optical emission spectroscopy and a collisional-radiative model. Plasma Sources Sci Technol 13:267–278